PHYSICAL REVIEW B VOLUME 35, NUMBER 6 15 FEBRUARY 1987-II

Temperature dependence of the high-frequency resistivity of a type-I superlattice due to impurity and phonon scatterings

X. L. Lei,* N. J. M. Horing, and J. Q. Zhang†

Department of Physics and Engineering Physics, Stevens Institute of Technology, Hoboken, New Jersey 07030

(Received 26 February 1986)

A general expression is developed here for the memory function of the linear dynamical conductivity of a type-1 superlattice with impurity and phonon scatterings, taking account of the electron-electron Coulomb interaction between different quantum wells as well as within a given quantum well. The real part of the frequency-dependent resistivity of a GaAs-$Al_xGa_{1-x}As$ quantum-well superlattice due to remote and background impurity scatterings and due to polar-optical-phonon couplings is calculated at several different temperatures, showing significant temperature dependence in both the bulk plasmon resonance (associated with close packing of the superlattice planes) and in the phonon resonance.

I. INTRODUCTION

The high-frequency linear conductivity of electrons in close-packed semiconductor superlattices[1,2] has attracted considerable interest recently. The scattering mechanisms discussed in the literature on this problem have been primarily those due to impurities or spatially separate mobile charge carriers, and the published studies have been limited to zero temperature. For elastic scattering mechanisms at $T=0$ K, we found a strong plasma resonance effect for the closely packed superlattice in Ref. 2. However, it is important to include the role of phonon scattering mechanisms in high-frequency transport calculations even at $T=0$ K, since the applied high-frequency electromagnetic field of the ac case does excite phonon contributions—in contrast to the case of linear dc transport, in which phonon-induced resistivity vanishes at zero temperature. A study of related high-frequency phonon effects, concerned with a single two-dimensionally confined system, has been reported in the literature.[3] Of course, our interest is focused on the superlattice with interlayer interactions.

Along with the inclusion of phonon scatterings in superlattice transport, we direct attention here to the role of finite temperature in the high-frequency resistivity. Since plasma resonance plays a decisive role in impurity-related high-frequency transport, and the Fermi level of the quasi-two-dimensional electron gas of a superlattice is generally low ($\leqq 100$ K for a carrier sheet density $N_s=2.5\times10^{11}$ cm^{-2}), a significant temperature variation in impurity-induced high-frequency resistivity is anticipated. Moreover, one must also expect temperature dependence arising from the Bose nature of the phonon distribution.

This paper is concerned with the determination of the temperature dependence of the dynamical resistivity of a type-I superlattice due to both impurity and phonon scatterings. In this, we take full account of electron-electron Coulomb interactions between different quantum wells ("interacting planes"), as well as within a given quantum well, in order to examine the temperature dependence of the "bulk" plasmon resonance characteristic of a close-packed type-I superlattice in the linear high-frequency resistivity. We also determine here the temperature dependence of resonant polar-optical-phonon excitations in the structure of the dynamic resistivity.

II. FORMULATION OF HIGH-FREQUENCY RESISTIVITY

It is well known that in a three-dimensional (3D) electron system, in which the electrons can be described by an effective-mass-approximation Hamiltonian in the absence of an electric field, the complex frequency-dependent linear resistivity $\rho(\omega)$ can be expressed in terms of a memory function $M(\omega)$ (Ref. 4) as

$$\rho(\omega)=-i\frac{m}{e^2n}[\omega+M(\omega)]\ , \qquad (1)$$

where e and m are the charge and effective mass of the carrier and n is its volume density. This formula is also valid for a two-dimensional (2D) electron gas if $\rho(\omega)$ is understood as the complex sheet resistivity $R(\omega)$ and n as the carrier sheet density N_s:

$$R(\omega)=-i\frac{m}{e^2N_s}[\omega+M(\omega)]\ . \qquad (2)$$

Moreover, this formula also describes the high-frequency resistivity $R(\omega)$ per sheet for a superlattice. Of course, the memory function $M(\omega)$, which includes all the information on linear high-frequency conductivity, depends on the system structure and scattering mechanisms, as well as on both interlayer and intralayer electron-electron interactions of the quantum-well superlattice. A high-frequency extension of the Lei-Ting description of transport[5–7] also provides a convenient basis for the derivation of the memory functions of various systems 3D, 2D, and superlattices with several scattering mechanisms (impurities and phonons). The role of superlattice geometrical structure has recently been elucidated in steady-state non linear dc transport.[7] In addition, we have studied superlattice structure in $M(\omega)$ for impurity scatterings,[2] and

 ©1987 The American Physical Society

we now extend this to include phonons, examining the temperature dependence of the memory function due to both scattering mechanisms for a superlattice having both interlayer and intralayer electron-electron interactions.

The system we will discuss in this report is a type-I superlattice, which consists of an infinite number of periodically arranged quantum wells of width a, and d is the spatial period or the distance between the two centers of adjacent layers. An $Al_xGa_{1-x}As$-GaAs-$Al_xGa_{1-x}As$ multilayer structure, in which the mobile electrons are in GaAs well regions, can be approximately described by such a model. We assume that (i) the potential wells are deep enough that tunneling can be neglected and the electrons confined to just one well, and (ii) the width of the well is narrow and the electron area density is not too high so that only the lowest subband is occupied. The wave function of the electron in the lth well can be written as

$$\psi_{l\mathbf{k}}(\mathbf{r},z)=e^{i\mathbf{k}\cdot\mathbf{r}}\zeta(z-ld) , \tag{3}$$

with energy $\varepsilon_{\mathbf{k}}=\hbar^2k^2/2m$, where m is the electron-band effective mass and $\mathbf{r}\equiv(x,y)$ and $\mathbf{k}\equiv(k_x,k_y)$ are 2D vectors in coordinate and momentum space, respectively, $k=|\mathbf{k}|$. The envelope function $\zeta(z)$ is nonvanishing only within the region $0<z<a$.

We are interested in the carrier transport parallel to the layer plane. To facilitate the study we introduce two-dimensional center-of-mass (c.m.) momentum $\mathbf{P}$ and coordinate $\mathbf{R}$ variables and separate them from the relative variables of the electrons. The system Hamiltonian H in terms of these c.m. variables and relative electron variables has been given in Ref. 7 and will not be repeated here.

When a uniform ac electric field of frequency ω,

$$\mathbf{E}=\mathbf{E}_m\cos(\omega t)=\mathbf{E}_m\,\mathrm{Re}(e^{-i\omega t}) , \tag{4}$$

is applied parallel to the plane, the small oscillation approximation for c.m. motion will be simple harmonic at the driving frequency[2,8]

$$\mathbf{R}(t)=\mathbf{R}_m\cos(\omega t+\phi)=\mathbf{R}_m\,\mathrm{Re}(e^{-i\omega t-\phi}) . \tag{5}$$

On the other hand, the force acting on the center of mass can be calculated from the statistical average

$$\langle\dot{\mathbf{P}}\rangle=-i\langle[\mathbf{P},H]\rangle/\hbar , \tag{6}$$

in which H is the Hamiltonian of the system, including c.m. interaction with the relative electron system through linearized impurity and phonon interactions, which are dynamically screened. The calculation involves an average of randomly distributed, spatially localized impurities, the evaluation of the phonon Green's function and the analysis of the electron density-density correlation function of the superlattice. We consider two different kinds of impurities: remote impurities and background impurities. The former are located in thin planar layers at a distance s from the center of each quantum well with equivalent charge number Z_r and sheet density N_r, and the latter are distributed uniformly within the well region with equivalent charge number Z_b and area density N_b per layer. We assume that there is no interference effect between different kinds of scatterers, so that the contributions to the frictional force due to the remote and background impurity scatterings are additive and averages over these two kinds of impurities can be done separately. The lattice vibrations in $Al_xGa_{1-x}As$-GaAs superlattices are considered to be the same as in bulk GaAs. The phonon normal modes are thus represented by a wave vector $\mathbf{Q}\equiv(\mathbf{q},q_z)$ and a branch index λ. $\Omega_{\mathbf{Q}\lambda}$ denotes the frequency of the corresponding normal mode and $M(\mathbf{Q},\lambda)$ represents the corresponding matrix element for electron-phonon scattering in 3D plane-wave representation. The contributions by different phonon modes are also additive, and thus can easily be included in a uniform formulation. The derivation parallels that of the nonlinear dc Lei-Ting force balance equation,[6–8] with the difference that we now have an exponential factor characteristic of the harmonic approximation of the form

$$e^{i\mathbf{q}\cdot[\mathbf{R}(t)-\mathbf{R}(t')]}\simeq 1+i\mathbf{q}\cdot\mathbf{R}_m[\cos(\omega t+\phi)-\cos(\omega t'+\phi)]=1+i\mathbf{q}\cdot\mathbf{R}_m\,\mathrm{Re}[e^{-i(\omega t+\phi)}(1-e^{-i\omega(t'-t)})] , \tag{7}$$

approximately expanded for small oscillations. Following the procedures of Ref. 5, we then obtain the force acting on the center of mass to the lowest order in R_m at any time t after the system has reached a steady oscillatory state as

$$\langle\dot{\mathbf{P}}\rangle=Ne\mathbf{E}_m\cos(\omega t)+\left[\frac{e^2}{2\varepsilon_0\kappa}\right]^2\sum_{\mathbf{q}}\frac{q}{q^2}(\mathbf{q}\cdot\mathbf{R}_m)\tilde{N}(q)\,\mathrm{Re}\{e^{-i(\omega t+\phi)}[\hat{\Pi}(0,\mathbf{q},0)-\hat{\Pi}(0,\mathbf{q},\omega)]\}$$
$$+\sum_{\mathbf{q},q_z,\lambda}|M(Q,\lambda)|^2\,|I(iq_z)|^2\,\mathbf{q}(\mathbf{q}\cdot\mathbf{R}_m)\,\mathrm{Re}\{e^{-i(\omega t+\phi)}[\Lambda(q_z,\mathbf{q},\lambda,0)-\Lambda(q_z,\mathbf{q},\lambda,\omega)]\} \tag{8}$$

(definitions of the quantities appearing here will be given below). Therefore, the equation of motion of the center of mass

$$\langle\dot{\mathbf{P}}\rangle=N_s m\ddot{\mathbf{R}}(t) \tag{9}$$

determines $\mathbf{R}_m$ and ϕ. It is convenient to write both the electric field and the current density in a complex form:

$$\mathbf{E}=\mathbf{E}_m e^{-i\omega t} ,$$
$$\mathbf{J}=N_s e\dot{\mathbf{R}}=\mathbf{J}_m e^{-i\omega t} .$$

For the system discussed, $\mathbf{J}$ and $\mathbf{E}$ are parallel and the complex scalar resistivity can be expressed as

$$R(\omega)\equiv\frac{E_m}{J_m}=-i\frac{m}{e^2N_s}[\omega+M^i(\omega)+M^p(\omega)] . \tag{10}$$

Here

$$M^i(\omega)=\frac{1}{mN_s\omega}\left[\frac{e^2}{2\varepsilon_0\kappa}\right]^2\sum_{\mathbf{q}}\frac{q_x^2}{q^2}\tilde{N}(q)[\hat{\Pi}(0,\mathbf{q},0)-\hat{\Pi}(0,\mathbf{q},\omega)] \quad (11)$$

is the impurity contribution to the memory function, and

$$M^p(\omega)=\frac{1}{mN_s\omega}\sum_{q,q_z,\lambda}|M(\mathbf{Q},\lambda)|^2|I(iq_z)|^2q_x^2\times[\Lambda(q_z,\mathbf{q},\lambda,0)-\Lambda(q_z,\mathbf{q},\lambda,\omega)] \quad (12)$$

is the phonon contribution to the memory function. In Eqs. (8) and (12) the imaginary part of Λ is

$$\Lambda(q_z,\mathbf{q},\lambda,\omega)=\hat{\Pi}_2(q_z,\mathbf{q},\omega-\Omega_{Q\lambda})\left[n\left[\frac{\hbar\Omega_{Q\lambda}}{k_BT}\right]-n\left[\frac{\hbar(\Omega_{Q\lambda}-\omega)}{k_BT}\right]\right]+\hat{\Pi}_2(q_z,\mathbf{q},\omega+\Omega_{Q\lambda})\left[n\left[\frac{\hbar\Omega_{Q\lambda}}{k_BT}\right]-n\left[\frac{\hbar(\Omega_{Q\lambda}+\omega)}{k_BT}\right]\right]. \quad (13)$$

Here $n(x/T)\equiv 1/(e^{x/T}-1)$ is the Bose function and $\hat{\Pi}(q_z,\mathbf{q},\omega)$ is the electron density-density correlation function of the superlattice,[7] which can be expressed in the random-phase approximation in the form

$$\hat{\Pi}(q_z,\mathbf{q},\omega)=\frac{\Pi(\mathbf{q},\omega)}{1-V(q,q_z)\Pi(\mathbf{q},\omega)}, \quad (14)$$

where $\Pi(\mathbf{q},\omega)$ is the two-dimensional density-density correlation function for a single sheet of electrons in the absence of the Coulomb interaction:

$$\Pi(\mathbf{q},\omega)=2\sum_{\mathbf{k}}\frac{f(\varepsilon_{\mathbf{k}+\mathbf{q}})-f(\varepsilon_{\mathbf{k}})}{\hbar\omega+\varepsilon_{\mathbf{k}+\mathbf{q}}-\varepsilon_{\mathbf{k}}+i\delta}, \quad (15)$$

in which $f(\varepsilon)=1/\{\exp[(\varepsilon-\mu)/k_BT]+1\}$ is the Fermi-Dirac function and μ is the chemical potential for electrons in a single quantum well. The effective Coulomb interaction is (neglecting the image charge contribution)

$$V(q,q_z)=\frac{e^2}{2\varepsilon_0\kappa q}[H(q)+S(q,q_z)], \quad (16)$$

where $S(q,q_z)$ comes from interlayer electron-electron interaction, exhibiting the characteristic superlattice structure factor

$$S(q,q_z)=\frac{\cos(q_zd)-\exp(-qd)}{\cosh(qd)-\cos(q_zd)}\exp(qa)I(q)^2. \quad (17)$$

The effective impurity sheet density is

$$\tilde{N}(q)=N_rZ_r^2\left[\frac{\cosh[q(d/2-s)]}{\sinh(qd/2)}\right]^2\exp(qa)I(q)^2+N_bZ_b^2\left[\frac{2}{qa}\frac{\exp(qa)-1}{\exp(qd)-1}I(q)+K(q)\right]^2. \quad (18)$$

In the above equations $H(q)$, $I(q)$, and $K(q)$ are form factors depending on the electron wave function within the well:

$$H(q)=\int\int e^{-q|z-z'|}\zeta(z)^2\zeta(z')^2dz\,dz',$$

$$I(q)=\int e^{-qz}\zeta(z)^2dz,$$

$$K(q)=\frac{1}{a}\int\int e^{-q|z-z'|}\zeta(z)^2dz\,dz'.$$

Taking the lowest subband envelope function as

$$\zeta(z)=\left[\frac{2}{a}\right]^{1/2}\sin\left[\frac{\pi z}{a}\right]\quad\text{for } 0<z<a,$$

we have ($u\equiv aq$)

$$H(q)=3\frac{1-\exp(-u)}{u^2+4\pi^2}+\frac{u}{u^2+4\pi^2}-\frac{1-\exp(-u)}{(u^2+4\pi^2)^2}\times(u^2-4\pi^2)+\frac{2}{u}\left[1-\frac{1-\exp(-u)}{u}\right], \quad (19)$$

$$I(q)=4\pi^2[1-\exp(-u)]/[u(u^2+4\pi^2)], \quad (20)$$

$$K(q)=\frac{8\pi^2}{(4\pi^2+u^2)u}\left[1+\frac{u^2}{4\pi^2}-\frac{1-\exp(-u)}{u}\right]. \quad (21)$$

III. RESULTS FOR IMPURITY SCATTERINGS

We have calculated the imaginary part of the impurity-induced memory function $M_2^i(\omega)$ at several different temperatures by using Eqs. (11), (14)–(18), and (19)–(21) for a GaAs-$Al_xGa_{1-x}As$ quantum-well superlattice with $a=100$ Å, $d=200$ Å, and carrier area density $N_s=2.3\times10^{11}$ cm^{-2} per layer. The scatterings are due to both remote and background impurities and the former are located at a distance $s=75$ Å from the center of each quantum well. We assume equality of the contributions of remote and background impurity scatterings to zero temperature dc resistivity. The material parameters used in the calculation are the electron-band effective mass $m=0.07m_e$ (m_e is the free-electron mass) and the GaAs static dielectric constant $\kappa=12.9$. The results at $T=0$ K, which have been discussed in detail in Ref. 2, are obtained using the well-known 2D zero-temperature expression for $\Pi(\mathbf{q},\omega)$ given by Stern.[9] For $T\neq0$ K, we perform numerical integration using the finite-temperature 2D expression for $\Pi(\mathbf{q},\omega)$ examined in Ref. 6. The results for $T=0$, 15, 40, 77, 150, and 300 K are plotted in Fig. 1. The most interesting feature is that resonance peaks around the bulk plasma frequency[10] $\omega_p=(e^2N_s/\varepsilon_0\kappa md)^{1/2}$ (associated with close packing of the superlattice planes) decrease significantly with increasing temperature. Nevertheless, the plasma resonance still shows up saliently in impurity-induced high-frequency resistivity even at room temperature.

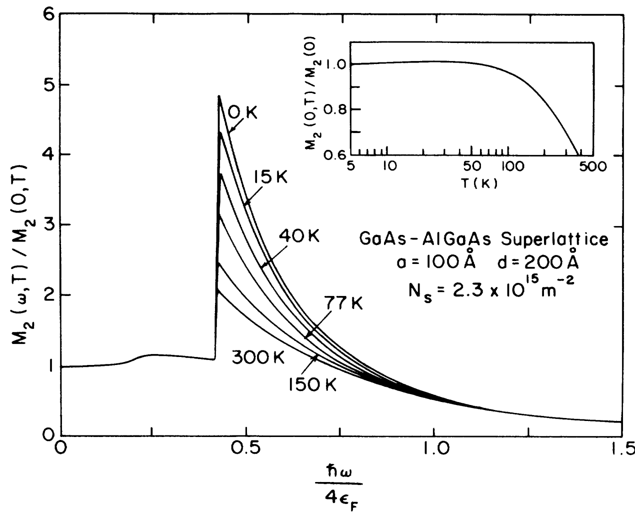

FIG. 1. Calculated $M_2(\omega,T)/M_2(0,T)$ due to remote and background impurity scatterings are shown as functions of $\hbar\omega/4\varepsilon_F$ at temperatures $T=0$, 15, 40, 77, 150, and 300 K for a GaAs-$Al_xGa_{1-x}As$ quantum-well superlattice with $a=100$ Å, $d=200$ Å, and $N_s=2.3\times10^{15}m^{-2}$. The contributions to dc resistivity by remote and background impurities are assumed 1:1 at $T=0$ K and the former are located at a distance $s=75$ Å from the center of each quantum well. The inset shows the temperature variation of $M_2(0,T)[M_2(0)\equiv M_2(0,0)]$. ε_F is the Fermi energy at zero temperature.

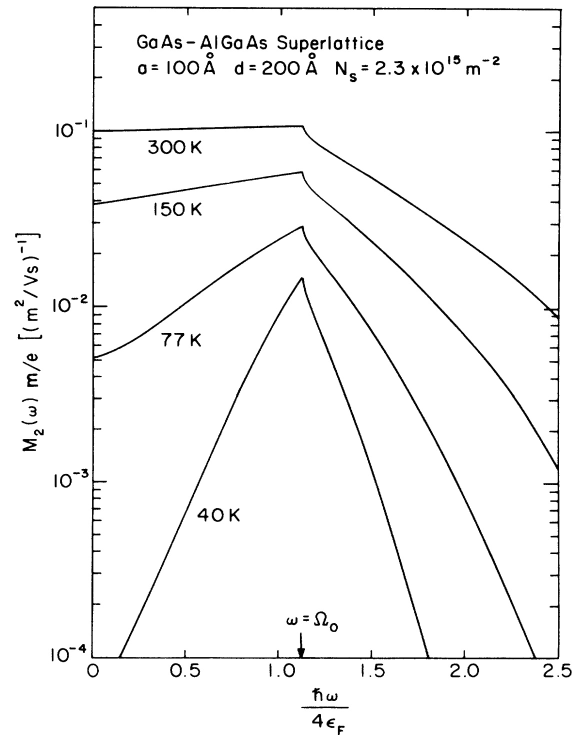

FIG. 2. Evaluations of $(m/e)M_2(\omega)$ due to polar-optical-phonon scattering are plotted as functions of $\hbar\omega/4\varepsilon_F$ at temperatures $T=40$, 77, 150, and 300 K for the same GaAs-$Al_xGa_{1-x}As$ superlattice as described in Fig. 1.

IV. POLAR-OPTICAL-PHONON CONTRIBUTION

In GaAs-$Al_xGa_{1-x}As$ systems, polar-optical phonons generally dominate the phonon-induced dc resistivity when temperature $T\geq50$ K. To examine their contribution to high-frequency resistivity we have calculated the imaginary part of the memory function due to polar-optical-phonon scattering. $M_2^{\xi}(\omega)$, using Eq. (12) at different temperatures for a GaAs-$Al_xGa_{1-x}As$ superlattice with $a=100$ Å, $d=200$ Å, and $N_s=2.3\times10^{11}$ cm^{-2}. Our evaluations of polar-optical-phonon-limited dynamical mobility are shown in Fig. 2, as functions of normalized frequency $\hbar\omega/4\varepsilon_F$ at $T=40$, 77, 150, and 300 K. For simplicity we assume a flat dispersion relation $\Omega_Q=\Omega_0$ for polar-optical phonons in the GaAs-$Al_xGa_{1-x}As$ system, and a Fröhlich interaction for electron-polar-optical-phonon coupling with $\hbar\Omega_0=3.54$ meV and high-frequency dielectric constant $\kappa_\infty=10.8$. $M_2^{\xi}(\omega)$ always increases with frequency from $\omega=0$ and reaches a maximum at $\omega\simeq\Omega_0$ before it decreases, reflecting the resonant excitation of polar-optical phonons by the high-frequency electric field. The peak of $M_2^{\xi}(\omega)$ at $\omega\simeq\Omega_0$, which is rather sharp at low temperature, becomes less significant at higher temperatures due to thermal excitation and smearing. Note that (i) effects of temperature dependence both in the Bose functions and in the electron density-density correlation functions of Eq. (13) have been taken into account, and (ii) effects of electron collective modes of the "interacting plane" superlattice have been carefully included in our numerical calculation. However, the latter yield an almost negligible (less than 2%) contribution to $M_2^{\xi}(\omega)$ for the system discussed. Moreover, for a weak polar material like GaAs, and at a carrier sheet density $N_s=2.3\times10^{11}$ cm^{-2} such that the bulk plasma frequency $\omega_p\simeq0.55\Omega_0$, the mixture of electron plasmons and polar-optical modes, thus the renormalization of phonon frequency, is unimportant.

ACKNOWLEDGMENTS

The authors wish to express their thanks to Professor J. L. Birman for helpful discussions. This work was partially supported by the U.S. Army (Electronic Materials Research Division) at the Electronics Technology and Devices Laboratory, Fort Monmouth, NJ 07703.

*Permanent address: Shanghai Institute of Metallurgy, Chinese Academy of Sciences, Shanghai, China.

†On leave from Shanghai Semiconductor Devices Company, Shanghai, China.

[1]N. Tzoar and C. Zhang, Phys. Rev. B 32, 1146 (1985).

[2]X. L. Lei, N. J. M. Horing, J. Q. Zhang, Phys. Rev. B 33, 2912 (1986).

[3]S. Das Sarma and A. Madhukar, Phys. Rev. B 22, 2823 (1980); X. Wu, F. M. Peeters, and J. T. Devreese, *ibid.* 34, 2621 (1986); also see T. Ando, A. B. Fowler, and F. Stern, Rev.

Mod. Phys. **54**, 437 (1982), and references cited therein.
[4]W. Götze and P. Wölfle, Phys. Rev. B **6**, 1226 (1972).
[5]X. L. Lei and C. S. Ting, Phys. Rev. B **32**, 1112 (1985).
[6]X. L. Lei, J. L. Birman, and C. S. Ting, J. Appl. Phys. **58**, 2270 (1985).
[7]X. L. Lei, N. J. M. Horing, and J. Q. Zhang, Phys. Rev. B **34**, 1139 (1986).
[8]N. J. M. Horing, X. L. Lei, and H. L. Cui, Phys. Rev. B **33**, 6929 (1986).
[9]F. Stern, Phys. Rev. Lett. **18**, 546 (1967).
[10]This bulk plasma frequency for a close-packed superlattice was first predicted by S. Das Sarma and J. J. Quinn, Phys. Rev. B **25**, 7603 (1982); also see A. C. Tselis and J. J. Quinn, *ibid.* **29**, 3318 (1984).